A new model for the self-trapped exciton in alkali halides

1991 J. Phys.: Condens. Matter 3 3125

(http://iopscience.iop.org/0953-8984/3/18/007)

J. Phys.: Condens. Matter 3 (1991) 3125–3138. Printed in the UK

A new model for the self-trapped exciton in alkali halides

A L Shluger†, R W Grimes and C R A Catlow
Davy Faraday Research Laboratory, The Royal Institution, 21 Albemarle Street, London W1X 4BS, UK

Received 15 November 1990, in final form 18 February 1991

Abstract. We report a quantum mechanical study of the structural and spectroscopic properties of the self-trapped exciton in LiCl. Our method interfaces the quantum cluster calculations on a $Li_{10}Cl_4$ cluster with a Mott–Littleton treatment of the relaxation of the surrounding lattice. Calculations on the V_k centre give structures that are in very good agreement with Mott–Littleton calculations, and yield optical absorption energies that compare well with experimental values. Our study of the triplet ground state of the self-trapped exciton reveals a minimum energy structure of C_{2v} symmetry caused by a small off-centre displacement (of $=0.07$ Å) of the Cl_2^- (V_k) ions which comprise the hole component of the exciton. The electron is in a largely delocalized state around the hole with both components localized more on the Cl ion that is displaced towards the perfect lattice site. The magnitude of the off-centre displacement is much less than in the earlier studies of Song *et al*. A key feature in the success of these calculations was the self-consistent polarization of the surrounding lattice to the quantum cluster.

1. Introduction

It is well known that irradiation of initially perfect alkali halide crystals results in the creation of self-trapped excitons. Experimentally, the most thoroughly investigated of such defects is the triplet ground state of the self-trapped exciton (TSTE). This is created after a cascade of non-radiative electronic transitions and/or vibrational relaxation. Further relaxation involves one of three processes: (i) the direct radiative transition to the crystal singlet ground state (excitonic luminescence), (ii) the relevant non-radiative transition; or (iii) the production of Frenkel defects [1, 2].

In order to understand the mechanisms of exciton self-trapping and the subsequent conversion of this species into primary radiation defects a number of studies have been carried out. Kabler [3] demonstrated experimentally that the distinctive triplet luminescence generated by fundamental excitation also arises when free electrons recombine with the self-trapped holes (V_k centre) [3]. The latter has been recognized as the hole component (core) of the TSTE. In addition, the atomistic structure of the V_k centre was uniquely established by electron nuclear double-resonance studies [4], as an X_2^- molecular ion oriented along a ⟨110⟩ axis in such a manner that it exhibits D_{2h} symmetry.

† Permanent address: Latvian State University, 19 Ranis Boulevard, 206098, Riga, USSR.

0953-8984/91/183125 + 14 $03.50

If we consider the self-trapped exciton ion to be generated by the trapping of an additional electron by a V_k centre, it might seem reasonable to assume that it has the same D_{2h} symmetry and atomistic structure as a V_k centre. This is the so-called on-centre or (V_k + e) model [5]. In previous investigations of this model, the wavefunction of the exciton electronic component was obtained by solving the Schrödinger equation for a single electron embedded in a pseudopotential of the X_2^- molecular ion and the crystalline field of the remaining crystal [6, 7]. The electronic configuration of the ground state of the TSTE was considered to correspond to the B_{3u} (A_{1g}, b_{3u}) state.

An alternative, off-centre TSTE model has been suggested by Block *et al* [8, 9]. The impetus for this model comes from optically detected magnetic resonance experiments on the TSTE in KCl which suggested that the two anions constituting the exciton hole core were non-equivalent. The off-centring concept was also used in Toyozawa's model [10] for the vibrational TSTE instability (with respect to the centre-of-mass shift) of the hole core (X_2^-) along a ⟨110⟩ axis. Further theoretical studies undertaken by Song *et al* [11–15] are based on the idea that the exciton off-centre structure is a consequence of the repulsion of the exciton electron by the electronic X_2^- pseudopotential. According to Song *et al* the electron is bound to the X_2^- molecular ion entirely as a result of the interaction with the crystalline field from the rest of the crystal which is created in regular sites from which two X_2^- anions are displaced. Thus, an electron tends to occupy one of the two empty sites created by its repulsion of the X_2^- ion from its on-centre (D_{2h}) configuration. The semi-empirical calculations of Song *et al* [11–15] yield very large TSTE centre-of-mass ⟨110⟩ displacements, reaching 2–6 au. In their model, the TSTE resembles more the F–H pair rather than $V_k + e^-$. Although this model can explain many of the experimental data relating to the properties of the self-trapped exciton [15], it cannot be verified directly by experiment. Moreover it is based on a rather simplified one-electron model. An advantage of the approach adopted by Song *et al* is the use of a flexible basis to describe the floating Gaussian functions for the exciton electron; however, their model did not permit the treatment of the electron and hole components of the exciton to the same level of accuracy. In particular, the approach used in their work does not allow an adequate calculation of the electron and V_k polarization when the latter is displaced along the ⟨110⟩ axis away from its symmetric position.

The first attempt at a many-electron calculation of the TSTE was undertaken by Stoneham [16]. However, computational restrictions required the use of a narrow basis applied to only four atoms, i.e. an Na_2Cl_2 cluster. Itoh *et al* [17] used the semi-empirical complete neglect of differential overlap (CNDO) method to investigate properties of the TSTE in KCl. They were able to demonstrate clearly the essential rôle that the V_k core electronic excitation had on permitting exciton barrierless translational motion. More recently, the modified INDO method has been used to study to the TSTE ground state in KCl [18]. This model included a self-consistent polarization treatment of the surrounding lattice. The calculation employed a basis of Slater-type atomic orbitals (AO) centred on crystalline ions and additional floating AOs necessary for a more flexible description of the delocalized wave function of the exciton electron. The intermediate neglect of differential overlap (INDO) calculations predict the adiabatic potential energy surface of the TSTE ground state to be flat with respect to a centre-of-mass displacement in ⟨110⟩ directions. Thus, within computational accuracy it was not possible to determine whether the energy surface has a minimum and therefore to define its symmetry. However, the calculated optical absorption energies of both electron and hole components as well as the π-luminescence band of the TSTE agree well with experiment, since they are predicted

to be weakly dependent on centre-of-mass displacement. The problem encountered with the INDO calculations is typical of semi-empirical INDO-type calculations with non-variational character of the AOs basis. In the present work, we overcome such problems by carrying out *ab initio* variational calculations of both the electronic structure and geometry of the TSTE in a LiCl crystal.

2. Method of calculation

In our calculations, the unrestricted Hartree–Fock–Roothaan equations [19] are solved for a molecular cluster embedded in a crystalline lattice. The embedding lattice consists of a set of point ions whose positions are allowed to relax around the defect. This model is formulated within the ICECAP code [20, 21].

An important consideration for an *ab initio* calculation is the choice of basis sets from which the wavefunctions of the valence electrons of the cluster are constructed. We have used valence portions of standard Gaussian contracted basis sets [22]—(3) for Li and (3/3) for Cl atoms respectively. The core electrons of the cluster Li^+ and Cl^- ions are described by semi-local Bachelet–Hamann–Schluter (BHS) [23] pseudopotentials. When simulating an exciton, the basis set must be extended to including additional floating Gaussian functions centred at interstitial positions. The centre points and Gaussian exponents of these AOs were optimized for each adiabatic surface point.

The response of the lattice outside the quantum cluster due to the incorporation of a defect within the quantum cluster is calculated using the Mott–Littleton methodology [24]. Thus, it is first necessary to replace the quantum cluster ions with conventional Born model ions.

The Mott–Littleton procedure is based upon a description of the lattice in terms of effective potentials. The crystal lattice is partitioned into two regions: an inner region I that, in this case, includes at its centre the replaced quantum cluster ions, and an outer region II which extends to infinity. In region I, interactions are calculated explicitly and all ions are relaxed to zero force. We consider interactions due to long-range Coulombic effects (assuming formal charges on all ions) and also short-range forces that are modelled using parametrized pair potentials. The response of region II is treated using the Mott–Littleton approximation [24].

The relaxed positions of the ions in region I are determined using a Newton–Raphson minimization technique. To ensure a smooth transition between regions I and II, we incorporate an interfacial region IIa in which the ion displacements are determined via the Mott–Littleton approximation but in which the interactions with the ions in region I are calculated by explicit summation. In the present calculations region I included 50 ions and region IIa extends out to 5.0 lattice units.

Long-range Coulombic interactions are summed using Ewald's method [24]. Short-range interactions between the perfect lattice ions were taken from [25] and modified until the equilibrium lattice parameter fitted the experimental value (5.1295 Å). The short-range parameters are reproduced in table 1.

Ion polarization effects are described using the shell model of Dick and Overhauser [25]. The model describes an ion in terms of a massless shell charge Y and a massive core of charge X. The formal charge state of an ion is therefore equal to $X + Y$. The core and shell charges are coupled by means of an isotropic harmonic spring of force constant k, so Y^2/k is the free-atom polarizability. Polarization of an ion can then occur through the displacement of the shell relative to the core.

Table 1. Mott–Littleton parameters.

Pair potentials	A (eV)	ρ (Å^{-1})	C (eV Å^6)
Cl^-–Li^+	1576.6	0.2792	0.0
Li^+–Li^+	1553.8	0.2164	0.0
Cl^-–Cl^-	1227.2	0.3214	10.34
$Cl^{(1/2)-}$–$Cl^{(1/2)-}$	11956.7	0.3339	1913.7
Shell parameters		Y (units of e)	k (eV Å^{-2})
Cl^-		−2.685	26.14
$Cl^{(1/2)-}$		−1.985	54.22
Li^+		0.0	—

In addition to giving a relaxation energy for the surrounding lattice the Mott–Littleton calculation will return a set of relaxed ion coordinates which can be used to define the positions of the point ions that embed the quantum cluster. It is important to note that ions which in the Mott–Littleton calculations are treated as polarizable are represented in the embedding array by the two charges X and Y displaced with respect to each other by the distance determined in the Mott–Littleton calculation. In this manner ion polarization effects are accounted for in the embedding region. Once the embedding charges are defined, the quantum cluster calculation can proceed. This yields the total cluster energy and, in addition, the charge density of the electrons in the cluster. Now, the charge density of this quantum cluster may deviate significantly from its representations by point ion charges that were previously used by the Mott–Littleton calculation. To correct for these inconsistencies, the difference in the electric field generated by the quantum cluster charge density and that produced by the point ion array is expanded as a multipole series. By including the field generated by the multipoles in the Mott–Littleton calculation, we can iterate between the quantum cluster and Mott–Littleton calculations until we reach multipole consistency. In this study, we restricted ourselves to the dipole and quadrupole terms.

The plan of our investigation was as follows: first we determined the equilibrium positions of the ions in the quantum cluster; these are displaced slightly from their perfect lattice sites due to the approximate nature of the boundary interactions between ions inside the cluster and the surrounding point ion array. Next, we calculated the electronic structure and optical absorption energies for the V_k centre which serves as the hole core of the exciton. Last we include an additional electron and study the adiabatic potential energy surface of the resulting TSTE.

3. Simulation studies

3.1. The perfect crystal

Due to the high computational cost of Hartree–Fock calculations, we are restricted in the number of ions in the quantum-mechanically-treated cluster. As we wish to study D_{2h} and C_{2v} exciton models (on-centre or off-centre, respectively), we have chosen to

use two clusters shown in figure 1—$[Li_{10}Cl_4]$ and $[Li_{10}Cl_8]$. Both clusters include the basis set AOs of the cations nearest to the central Cl_A^-–Cl_A^- quasimolecule (see figure 1). This is important as it allows the extended (non-point) nature of these ions to be modelled.

Since we are studying a strongly ionic material, the total number of valence electrons in the cluster $[Li_{10}Cl_4]$ is 32. Only the AOs centred on the regular ions were included in the basis sets for the perfect crystal calculations.

The equilibrium positions obtained for the perfect crystal cluster ions are given in table 2. We note that the cluster boundary ions were displaced whereas the two central Cl^- ions that are coordinated by six nearest-neighbour cluster ions are practically undisplaced. The small size of the central ion displacements suggests that our cluster model is appropriate. The same result is obtained when floating functions (as employed in later calculations which involve the exciton) are included into the basis set.

3.2. The singlet-to-triplet excitation of the perfect crystal

To estimate the initial excitation energy necessary to form an exciton, we have calculated the difference between the total energies of the singlet (ground) and triplet (excited) states of the $[Li_{10}Cl_4]$ perfect crystal cluster. In both cases, the ionic cores inside and outside the cluster were fixed in the lattice sites corresponding to the crystal equilibrated in the singlet state; that is, we are describing a Franck–Condon transition and allow only electronic polarization (modelled by shell displacements) in the crystal excited state. Using this model we calculated an excitation energy of 9.6 eV, which is close to the experimental value of 8.67 eV [27].

The influence of the cluster size on the calculated results must be carefully considered. Thus, we carried out several calculations using the larger $[Li_{10}Cl_8]$ cluster (figure 1). The inclusion of four additional Cl^- anions (Cl_c: see figure 1) reduced displacements of the surround Li^+ cations (Li_3) but the electronic structure of the cluster and its excitation energy (9.7 eV) remain unchanged.

3.3. The V_k centre

Since the V_k centre (self-trapped hole) is positively charged with respect to the perfect crystal, calculations of its structure and properties require the self-consistent incorporation of the crystal polarization. The ICECAP code is therefore an ideal tool to investigate such a defect as it integrates the effect of long-range polarization with a quantum mechanical description of the Cl_2^- pseudo-molecule. To perform such calculations, it is necessary for the initial Mott–Littleton part of the calculation to provide a short-range interaction that will describe the interaction between the two $Cl_A^{(1/2)-}$ ions (see figure 1) that constitute the Cl_2^- molecule. In this study we used the same Cl_A–Cl_A potential as has been used in previous studies of the V_k centre [28]. This provides a good representation of the interatomic potential determined from Hartree–Fock calculations for the Cl_2^- molecule [30]. We note that the same Hartree–Fock generated potential has been used as the basis for the derivation of other potential forms for the Cl_2^- molecule [31].

In addition to a Cl_A–Cl_A potential it is also necessary to define short-range potentials between the Cl_A ions that have non-integral net charges and other ions of the crystal whose charges are ± 1 (i.e. between Cl_A and Cl^-; Cl_A and Li^+). We followed the procedure in [28], and we used the same short-range interactions between the quantum

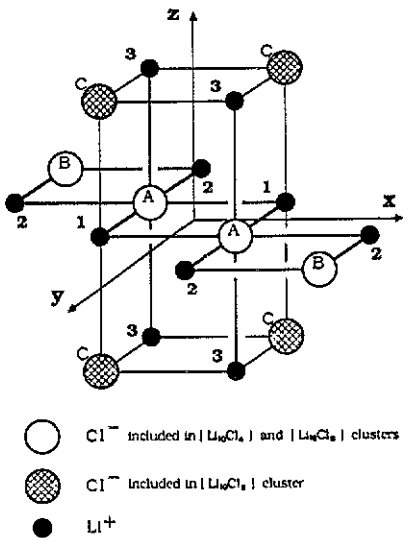

Figure 1. The cluster of atoms treated quantum mechanically in the ICECAP calculations of the TSTE.

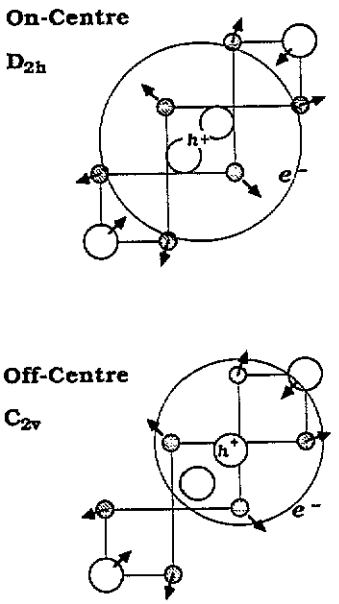

Figure 2. Schematic representation of the on-centre (D_{2h}) and the off-centre (C_{2v}) models of the TSTE. The large circle represents the delocalized trapped electron; h^+ is the hole component.

cluster ions and the rest of the crystal as between ions in the regular lattice sites. The validity of this approximation was investigated by comparing the V_k centre geometries in LiCl calculated using a purely Mott–Littleton methodology employing the CASCADE code [29]. Two sets of parameters for the pair interaction of the $Cl_A^{(1/2)-}$ defect ions with regular lattice ions were used. The first parametrization is the same as was described above—that is, the Cl_A–Cl^- and Cl_A–Li^+ potentials are approximated by the Cl^-–Cl^- and Cl^-–Li^+ perfect lattice potentials. In the second case the Cl_A–Cl^- and Cl_A–Li^+ potentials were those that had been determined explicity [31] in a previous investigation. In both cases the Cl_A–Cl_A potential was one that, as discussed above, had been determined by fitting to the results of the *ab initio* calculation [30].

The displacements of the ions in figure 1 away from their perfect lattice sites calculated using the purely Mott–Littleton approach (potential models A and B) are compared in table 2 with those positions determined using the quantum cluster ICECAP code. The closeness of the results of the two Mott–Littleton calculations suggests that our simplification regarding the equivalence of the Cl_A–Cl^- and Cl_A–Li^+ potentials with Cl^-–Cl^- and Cl^-–Li^+ potentials is justified.

The closeness of the results obtained using the Mott–Littleton methodology to the ICECAP values (see table 2) demonstrates the usefulness of the pair-potential method in investigating these types of defect centres in ionic crystals. However, a quantum mechanical approach allows us to obtain information about the spectroscopic characteristics of the V_k centre which are beyond the scope of the Mott–Littleton approach. This includes optical and magnetic resonance parameters [32]. In the present study we have calculated only the V_k centre optical transition energies. Our calculations predict the energies of the optical $\sigma_g \rightarrow \sigma_u$ and the $\pi_g \rightarrow \sigma_u$ transitions to be 3.6 eV and 1.8 eV,

Table 2. Ion coordinates in the released perfect lattice and the displacements due to V_k-centre formation. The results for ICECAP and CASCADE calculations are in units of the lattice constant, $a = 2.5648$ Å; a positive value corresponds to outward displacement.

Ion type	Ideal lattice			ICECAP relaxed perfect lattice			V_k centre								
							ICECAP			CASCADE with pair potentials [27]			CASCADE with pair potentials [29]		
A	0.50	0.50	0.00	0.495	0.495	0.00	−0.115	−0.115	0.00	−0.114	−0.114	0.00	−0.115	−0.115	0.00
B	1.50	1.50	0.00	1.465	1.465	0.00	−0.01	−0.01	0.00	−0.020	−0.020	0.00	−0.020	−0.020	0.00
C	−0.50	0.50	1.00	−0.50	0.50	1.00	0.00	0.00	0.00	0.005	0.005	0.00	0.002	0.002	0.009
1	−0.50	0.50	0.00	0.46	0.46	0.00	0.12	0.12	0.00	0.107	0.107	0.00	0.042	0.042	0.00
2	1.50	0.50	0.00	1.46	0.53	0.00	0.10	0.01	0.00	0.066	0.002	0.00	0.067	−0.003	0.00
3	0.50	0.50	1.00	0.50	0.50	0.57	0.00	0.00	0.06	−0.006	−0.006	0.067	−0.006	−0.006	0.055

Table 3. Coordinates and exponents of the three different sets of floating functions (FOs) used to calculate the total energy of the on-centre TSTE.

Basis set	Type of GF	Number of GFs	Coordinates of GFs for on-centre TSTE	Values of optimized exponents	Total energy for on-centre TSTE (eV)	Total energy for off-centre TSTE (eV)
4 FOs	φ_1	2	(±1.00; ±1.00; 0.00)	0.08	−1588.4	−1588.3
	φ_2	2	(0.00; 0.00; ±0.50)	0.083		
10 FOs	φ_1	2	(±0.95; ±0.95; 0.00)	0.08	−1588.81	−1588.96
	φ_2	8	(±0.95; ±0.04; ±0.50)	0.077		
14 FOs	φ_1	4	(±0.95; ±0.95; ±0.50)	0.08		
	φ_2	8	(±0.95; ±0.04; ±0.50)	0.077	−1589.22	−1589.37
	φ_3	2	(±0.00; ±0.00; ±0.50)	0.077		

respectively, the former of which compares well with the previous experimental values of 3.16 eV (the $\pi_g \rightarrow \sigma_u$ transition is too weak to be observed experimentally) [4]. We also calculated a value of 1.9 eV for the $\pi_u \rightarrow \sigma_u$ transition which is close to experimental value of 2.09 eV determined from electron paramagnetic resonance studies [4].

3.4. The TSTE ground state

The central purpose of the present paper is to study theoretically both on-centre and off-centre models of the TSTE (see figure 2). We shall first study the electronic and atomic structures of the on-centre excitons; then, using the same quantum cluster we will calculate the adiabatic surface with respect to a series of fixed displacements of one of the Cl_A anion along the ⟨110⟩ axis but allowing complete relaxation of all other ion coordinates. All calculations are carried out for the triplet state of the $(Li_{10}Cl_4)$ cluster. Localization of the exciton electron is guaranteed by the presence of the hole component; that is, of the V_k centre.

The results for the V_k centre demonstrate that the basis set of AOs that we used, despite being rather restricted, allows us to reproduce the geometry and the optical absorption of the hole core of the exciton. However, the basis is too narrow to describe successfully the wave function of the excited electron component of the exciton. To increase the flexibility, additional Gaussian orbitals were included into the basis set. These so-called floating functions (FOs) were centred on interstitial positions. The advantages of using FOs was demonstrated earlier by Song *et al* [11–15]. In choosing the number and symmetry of the FOs we tried to ensure that the resulting basis set was able to describe the density distribution of the exciton electron in the D_{2h} symmetry and the polarization of the electron and hole components of the TSTE when the V_k core is shifted and the exciton symmetry is reduced.

3.4.1. The on-centre TSTE. Parameters of the three different FO basis sets used in modelling the on-centre exciton are presented in table 3. The largest coefficients of the molecular orbital expansion of the excited electron over the AOs of the basis set are given in table 4. We present such results only for the 10- and 14-FO bases. For both of these on-centre calculations one can see that the one-electron wave function for the exciton electron is delocalized over the whole quantum cluster (this is represented in figure 2 by

the large circle). We found that splitting the single-FO Gaussian, φ_1, of the 10-FO basis set into two functions and thus extending the basis set up to 14 FOs did not change the total contribution of these orbitals to the electron wave function. However, much greater quantitative changes in expansion coefficients of MOs arise when φ_3-orbitals are added. Nevertheless, the qualitative character of the wave function and the one-electron energy are not strongly affected (see table 4).

As the basis set is extended, the total energy of the crystal containing the TSTE (including the crystal polarization energy) is reduced (see table 3). However, there is no indication of convergence to a constant value. As our calculations did not include the Kunz–Klein localizing potential [33], further basis extension could lead to the complete exciton electron delocalization due to the absence of any Pauli repulsion from the electronic shells of ions surrounding quantum cluster. Despite the fact that this produces an unspecified uncertainty in our calculations, because of the localized nature of FOs we expect the error to be small, and almost certainly it does not affect our qualitative conclusions. The optimized FO exponents that we found are close to those of the most occupied FOs in the wider basis set used by Song [34] in calculations of the TSTE carried out using an extended ion method [11].

The basis set extension by FOs does not significantly affect the geometry of the cluster simulating the perfect crystal. We also found that the displacements of ions in the quantum cluster describing the on-centre TSTE do not depend on the number of FOs. The magnitude of the ion displacements calculated using the 10-FO basis set are shown in table 5. They are close to or coincide with analogous displacements of all V_k centre ions except for Li_3. The distance between Cl_A ions remains almost the same as in the V_k centre, and this dictates the displacements of the Cl_B, Li_1 and Li_2 ions. A partial screening of the V_k charge by the TSTE electron results in a reduced Li_3 displacement.

The total Mulliken populations for the 10-FO basis set, which are reported in table 5, give us valuable information concerning the relative charge distribution for the D_{2h} exciton. From this, it was realised that to calculate multipole moments in the defect region and the Coulomb interaction of Cl_A, and Cl_B anions with ions outside the cluster, it is necessary to use charges of these two types of ion equal to $-0.5e$ and $-0.8e$ respectively.

The main effect of the FO basis set on the on-centre TSTE electronic structure is to change the one-electron energy of the exciton electron and its density redistribution. For example, as the number of FOs increases from 4 to 10, the one-electron energy decreases by 1.4 eV. This is accompanied by exciton electron density delocalization. After increasing the FO basis to 14 functions, the energy level value decreases only by a further 0.33 eV (see table 4).

3.4.2. The off-centre TSTE. In order to simulate the reduction in the TSTE symmetry from on-centre (D_{2h}) to off-centre (C_{2v}) one of Cl_A anions was displaced along the ⟨110⟩ axis, with simultaneous total energy minimization with respect to all other ion positions and FO parameter optimization. The electronic density distribution and adiabatic surface obtained for the on–off-centre displacement depends essentially on the flexibility of the basis set used (in this case 4, 10 or 14 FOs). For the extended bases of 10 and 14 FOs the results are essentially the same. When passing from the on-centre to the off-centre configuration the minimum in the energy in both cases occurs at a Cl_A–Cl_A centre-of-mass displacement of $\simeq 0.07$ Å. With this displacement the total energy has been reduced by $\simeq 0.15$ eV (see figure 3). In table 5 we report, for the 10-FO basis set, both the displacements of the quantum cluster ions at the C_{2v} exciton adiabatic potential energy

Table 4. The one-electron energy and the expansion coefficients of the component Gaussian basis set functions of the exciton electronic component (the positive functions (e.g. φ_1^+) are closer to the off-centre (C_{2v}) hole comonent of the displaced exciton). Their larger coefficients indicate that the diffuse electron is centred around the hole component.

Basis sets	Symmetry	One-electron energy (eV)	φ_1^-	φ_1^+	φ_2^-	φ_2^+	φ_3	$Cl_a^-(3s)$	$Cl_a^+(3s)$	Li_1	Li_2^-	Li_2^+	Li_3^-	Li_3^+
14 FOS	D_{2h}	−1.58	−0.18	−0.18	0.04	0.04	−0.17	0.27	0.27	0.36	0.08	0.08	0.25	0.25
10 FOS	D_{2h}	−1.25	−0.16	−0.16	0.05	0.05	—	0.32	0.32	0.26	0.15	0.15	0.17	0.17
14 FOS	C_{2v}	−1.68	−0.05	−0.21	−0.01	0.16	−0.09	0.16	0.41	0.27	0.02	0.15	0.16	0.32
10 FOS	C_{2v}	−1.44	−0.06	−0.19	−0.02	0.14	—	0.20	0.39	0.22	0.06	0.22	0.09	0.20

Table 5. Relative displacements and Mulliken populations of the quantum mechanical cluster ions in on-centre and off-centre TSTE positions.

Ion type	On-centre (D_{2h})				Off-centre (C_{2v})			
	Relative displacement of ions			Mulliken populations of ions	Relative displacement of ions			Mulliken populations of ions
	Δx	Δy	Δz		Δx	Δy	Δz	
Cl_A^-	−0.113	−0.113	0.00	7.255	−0.430	−0.130	0.00	7.441
Cl_A^+	−0.113	−0.113	0.00	7.255	−0.085	−0.085	0.00	7.045
Cl_B^-	−0.025	−0.025	0.00	7.685	−0.005	−0.005	0.00	7.695
Cl_B^-	−0.025	−0.025	0.00	7.685	−0.005	−0.005	0.00	7.667
Li_1	0.012	0.012	0.00	0.188	0.130	0.140	0.00	0.142
Li_2^-	0.10	0.001	0.00	0.0838	0.090	0.00	0.00	0.032
Li_2^+	0.10	0.001	0.00	0.0838	0.110	0.00	0.00	0.139
Li_3^-	0.00	0.00	0.00	0.0847	0.00	0.00	0.00	0.027
Li_3^+	0.00	0.00	0.00	0.0847	0.00	0.00	0.00	0.117

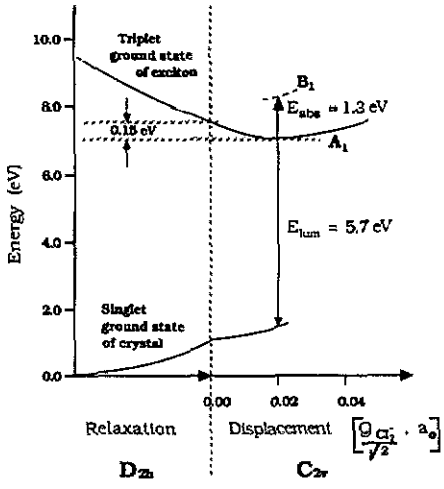

Figure 3. An energy diagram of the TSTE relaxation to its electronic ground state and subsequent annihilation to the crystal singlet ground state.

surface minimum and the net electron populations. As with the on-centre examples, we find that the one-electron wave function is delocalized over the whole quantum cluster (see table 4). These results also clearly predict that both the electron and hole components of the exciton are localized more on the Cl_A ion which is closest to the perfect lattice site. The relevant exciton model is shown schematically in figure 2.

A key component in these calculations is the polarization of the surrounding lattice as this tends to promote our localization model. However, since the polarization is self-consistent with respect to the electronic field of the quantum cluster ions we can discount the notion that our model is simply a consequence of the lattice polarization dictating the positions of the ions in the quantum cluster since the quantum cluster ions in their turn influence the lattice polarization.

Calculations employing the inferior 4-FO basis set predict that the total energy of the system will increase as the Cl_A anion is displaced from the on-centre site. In addition, the TSTE electron and hole polarization are small and behave in the opposite way to that shown in figure 2. For example, if the Cl_A–Cl_A centre-of-mass is displaced by 0.07 Å, the electron population of the Cl_A anion, closest to its lattice site, increases by 0.06*e* while the population of the other Cl_A anion is reduced by the same amount. This displacement increases the total energy of the system by 0.1 eV. The electron redistribution calculated using this smaller FO basis correspond more closely to the model proposed by Song *et al*

It appears that as the exciton moves to the off-centre position, the change in total energy is very slight and the qualitative behaviour (i.e. increase/decrease) can depend on whether sufficient attention has been paid to the parameters used in the method of calculation.

Figure 3 summarizes schematically our main results concerning the formation energy of the TSTE and its optical properties. We calculated the optical absorption energy corresponding to the $A_1 \rightarrow B_1$ transition of the TSTE electronic component to be 1.3 eV. This is smaller than the experimental value of 2.1 eV [35]. Conversely, our calculated π-luminescence energy of 5.7 eV is larger than the experimental value of 4.18 eV [36]. This could result from an overestimated exciton excitation energy (9.6 eV compared with the experimental value of 8.67 eV [27]) which may itself be due to the fact that we

used an unoptimized cation basis set. We expected basis optimization to reduce the adiabatic surface as a whole and thus give a better agreement between calculated and experimented optical transition energies.

Lastly, we note that the calculated net electron populations of Li_1^+ and Li_2^+ cations are close to those for Li_3^+ (see table 5). The same is also true for the spin populations of these ions. This is in good agreement with conclusions of ESR studies of the TSTE in KCl [8, 9], which indicate that the symmetry of the spin density distribution of the TSTE electron component is close to that of the F centre.

4. Summary

The results presented above indicate that the TSTE in the alkali halide LiCl is unstable in its ground state with respect to the centre-of-mass displacement from the on-centre to off-centre position. That is, we predict a reduction in exciton symmetry from D_{2h} to C_{2v}. However, unlike in the calculations of Song *et al* [11–15, 37], our displacement and total energy gain are rather small. Our qualitative model of the polarization of the electron and hole components is also different from the models of Song *et al*. This difference results almost certainly from the self-consistent treatment of the mutual polarization of the electron and hole components of the exciton. However, another contributory factor could be the mixed character of the one-electron wave function of the TSTE electron predicted in the present study. Our work suggests that the cation AOs serve to stabilize the one-electron energy of the TSTE electron component. This point plays a decisive rôle in the small reduction of the total energy as the TSTE moves to the off-centre position. A comparison of the results obtained when making use of different FO basis set shows that the character of the exciton polarization is a consequence of FO basis set symmetry and flexibility. We note that the 10- and 14-FO basis sets reproduce some aspects of the symmetry of anion d-type atomic orbitals. The extension of the anion basis set by including d orbitals might therefore be important in future investigations. Lastly, we note that although the results of these calculations are specific to LiCl, the results of preliminary calculations suggest that a similar model will be appropriate for describing the behaviour of excitons in other alkali halides.

Acknowledgments

The authors wish to thank the Ministry of Education, Latvian Republic and AEA Technology, Harwell for financial support. The authors are grateful to N Itoh, J H Harding, A H Harker, A M Stoneham and A Testa for help and valuable discussions. Thanks are due to R G Bell for his help in the computational work.

References

[1] Itoh N 1982 *Adv. Phys.* **31** 491
[2] Lushchik Ch B and Lushchik A Ch 1989 *Decay of Electronic Excitations with Defect Formation in Solids* (Moscow: Nauka)
[3] Kabler M N 1969 *Phys. Rev.* **136** A4256
[4] Schoemaker D 1972 *Phys. Rev.* B 7 786

[5] Fowler W B, Marone M J and Kabler M N 1973 *Phys. Rev.* B **8** 5909
[6] Song K S, Stoneham A M and Harker A H 1975 *J. Phys. C: Solid State Phys.* **8** 1125
[7] Itoh N, Stoneham A M and Harker A H 1977 *J. Phys. C: Solid State Phys.* **10** 4197
[8] Block D, Wasiela A and Merle d'Aubigne Y 1978 *J. Phys. C: Solid State Phys.* **11** 4201
[9] Block D and Wasiela A 1979 *Solid State Commun.* **28** 455
[10] Toyozawa Y 1977 *J. Phys. Soc. Japan* **43** 4286
[11] Leung C, Brunet G and Song K S 1985 *J. Phys. C: Solid State Phys.* **18** 4459
[12] Williams R T, Song K S, Faust W L and Leung C H 1986 *Phys. Rev.* **33** 7232
[13] Song K S, Leung C H and Williams R T 1989 *J. Phys.: Condens. Matter* **1** 683
[14] Song K. S and Leung C H 1989 *J. Phys.: Condens. Matter* **1** 8425
[15] Song K S and Leung C H 1990 *Rev. Solid State Sci.* **4** 357
[16] Stoneham A M 1974 *J. Phys. C: Solid State Phys.* **7** 2776
[17] Itoh N, Stoneham A M and Harker A H 1977 *J. Phys. C: Solid State Phys.* **10** 4197
[18] Shluger A L 1990 unpublished
[19] Metzgar T D and Bloor J E 1974 *Quantum Chemistry Program Exchange* **11** 234
[20] Vail J M, Harker A H, Harding J H and Saul P 1984 *J. Phys. C: Solid State Phys.* **17** 5401
[21] Harding J H, Harker A M, Keegstra P B, Pandey R, Vail J M and Woodward C 1985 *Physica* B **131** 151
[22] Huzinaga S 1984 *Gaussian Basis Sets for Molecular Calculations* (Amsterdam: Elsevier)
[23] Bachelet G R, Hamann D R and Schluter M 1982 *Phys. Rev.* B **26** 4199
[24] This technique has been reviewed in
J. Chem. Soc. Faraday Trans. II **85** 1989 special issue ed C R A Catlow and A M Stoneham
[25] Catlow C R A, Diller K M and Norgett M J 1977 *J. Phys. C: Solid State Phys.* **10** 1395
[26] Dick B G and Overhauser A W 1958 *Phys. Rev.* **112** 90
[27] Teegarden K and Baldini G 1967 *Phys. Rev.* **155** 896
[28] Cade P E, Stoneham A M and Tasker P W 1984 *Phys. Rev.* B **30** 4621
[29] Leslie M 1982 *SERC Daresbury Laboratory Report* DL/SCI/TM31T
[30] Gilbert T L and Wahl A C 1971 *J. Chem. Phys.* **55** 5247
[31] Catlow C R A, Diller K M and Hobbs L W 1980 *Phil. Mag.* A **42** 123
[32] Pandey P and Kunz A B 1988 *Phys. Rev.* B **38** 10150
[33] Kunz A B and Klein D L 1978 *Phys. Rev.* B **17** 4614
[34] Song K S 1990 private communication
[35] Tanimura K 1990 private communication
[36] Pooley P and Runciman W A 1970 *J. Phys. C: Solid State Phys.* **3** 1815
[37] Baetzold R C and Song K S 1991 *J. Phys.: Condens. Matter* **3** 2499